https://doi.org/10.26552/com.C.2001.2-3.68-75

kamUNikácie
COMMUNICATIONS

Manfred Depenbrock – Christian Foerth – Frank Hoffmann – Stefan Koch – Andreas Steimel – Markus Weidauer *

RIADENIE RÝCHLOSTI ASYNCHRÓNNEHO MOTORA S ORIENTÁCIOU NA STATOROVÝ TOK BEZ SNÍMAČA PRE TRAKCIU

SPEED-SENSORLESS STATOR FLUX-ORIENTED CONTROL OF INDUCTION MOTOR DRIVES IN TRACTION

Nepriame riadenie statorových kvantít (Indirect Stator Quantities Control - ISC) kombinuje v sebe princíp orientácie na statorový tok, úspešne overený ako priame momentové riadenie (Direct Self-Control) s impulzne šírkovou moduláciou (PWM). Tým sa dosahuje vysoká dynamika momentu a robustné chovanie odolné voči napäťovým poruchám v celom operačnom rozsahu vrátane oblasti zoslabovania budenia. Po starostlivej korekcii chýb v napätí striedača sa rozdiel v priestorových vektoroch statorových prúdov motora a modelu používaného v riadení využíva na odhad rýchlosti, čo dovoľuje odstrániť snímač rýchlosti. Špeciálne riadenie toku dovoľuje nekonečne pomalú zmenu medzi trakčným a brzdným režimom.

Indirect Stator-Quantities Control (ISC) combines the principle of stator flux-orientation proven successful in Direct Self Control (DSC) with Pulse Width Modulation (PWM). High torque dynamics and robust behavior against input voltage disturbance are achieved in the whole operation range including field-weakening. After careful correction of inverter voltage errors the difference of the stator current space vectors in the machine and in the control model is employed for speed estimation, allowing dispensing with speed sensors. A special flux management allows an infinitely slow change between driving and braking.

1. Introduction

In the 1980's Vector Control of Induction Machine,successful with industrial drives, already was introduced in traction[1]. It impresses the components of the stator current space vector in orientation to the rotor flux space vector by means of control. In high power traction drives this approach was limited; as the switching frequency is, in general too low to sufficiently impress; the current.

In 1984 M. Depenbrock proposed ([2]) orienting the space vector of the stator voltage directly to the space vector of stator flux, which is obtained in a very simple manner as the integral of the stator voltage, according to Faraday's Law. In Direct Self Control (DSC) the stator flux activates the suited next voltage switching when it reaches predetermined thresholds. Thus it guides itself on its trajectory and controls the magnetization of the machine. Torque is controlled by the track speed in DSC by extremely simple means of a torque hysteresis controller which guides pulsing and makes a separate Pulse Width Modulator unnecessary. Flux Self Guidance makes the drive insensitive to input voltage disturbations that are met typically in traction, as e.g. by pantograph bouncing. Asynchronous pulsing exploits the limited switching frequency best compared to synchronized pulse patterns [3] used elsewhere.

In the nineties IGBT inverters thrusted aside GTO inverters in the range of low and medium powers typical for Light Rail applications, allowing distinctly higher switching frequencies. The question arose how to transfer the advantages of Direct Stator Flux Control to these new inverters which made some of the old restrictions obsolete. With a sufficient ratio of switching to stator base frequency sinusoidal PWM can be used without any drawback, making the traction drive easier to adapt to severe line harmonics limitations. It was already employed with DSC-controlled GTO inverters in the starting region [4] where DSC shows some complications [1].

As Stator Flux-Oriented Control already uses the complete machine model it can be well applied for estimation of speed from

* [1]Prof emer. Dr.-Ing. Manfred Depenbrock, Prof. Dr.-Ing. Andreas Steimel, [2]Dipl.-Ing. Christian Foerth, Dr.-Ing. Frank Hoffmann, Dr.-Ing. Markus Weidauer, [3]Dr.-Ing. Stefan Koch
[1]Institute for Generation and Application of Electric Energy, Ruhr-University Bochum, D-44780 Bochum,
Tel.: ++49-234-32-23890, Fax: ++49-234-32-14597, E-mail: sekretariat@eaee.ruhr-uni-bochum.de
[2]Siemens TS GTE 3, Postbox 3240, D-91050 Erlangen, Tel.: ++49-9131-7-35151, Fax: ++49-9131-7-32952, E-mail: frank.2.hoffmann @ts.siemens.de;
[3]Siemens A&D LD B E 5, Tel.: ++49-9131-7-34722, Fax: ++49-9131-7-32952 E-mail: stefan.koch@erl£siemens.de.
Correspondence to Prof. Dr.-Ing. A. Steimel

the terminal quantities. As additional broadband voltage sensors are often not wanted a careful compensation of the inverter errors is necessary when the voltage is modeled from measured DC link voltage and switching commands. But then robust observers schemes can be applied to estimate two parameters, e. g. the speed and stator resistance, from the difference of the space vectors of machine and model current. As the model is of the linear fundamental type the system is in principle unobservable at stator frequency equal zero. Special management of the flux magnitude enables the drive to operate permanently at any speed around zero.

2. Model of the Machine

Each highly dynamic flux-oriented control needs a model of the induction machine as exact as possible in order to calculate non-measurable fluxes. On the other hand, it must be calculable by a Digital Signal Processor (DSP) in sufficiently short time. Space Vector (SV) notation [5] is, as most commonly used for description, denoted by arrows under the symbol. For the stator-flux-orientation the "canonical" Γ - Equivalent Circuit Diagram (ECD) (with the leakage inductance concentrated in the rotor mesh) using the stator-fixed reference system is most convenient (Fig. 1):

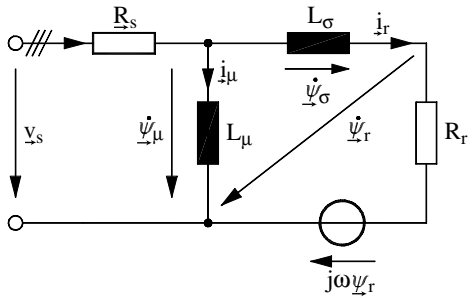

Fig. l. Equivalent Circuit Diagram of induction machine in Space Vector notation, stator-fixed reference frame

It correctly describes the fundamental values of all quantities. Saturation of the main inductance L_μ is measured off-line and taken into account by a characteristic dependent on stator flux magnitude. The stator resistance R_S must be identified on-line.

The state equations can be derived according to this ECD:

$$\dot{\underrightarrow{\psi_\mu}} = \underrightarrow{v_s} - R_s \cdot \underrightarrow{i_s} \tag{1}$$

$$\dot{\underrightarrow{\psi_r}} = R_r \cdot \underrightarrow{i_r} + j \cdot \omega \cdot \underrightarrow{\Psi_r} \tag{2}$$

The stator current is:

$$\underrightarrow{i_s} = \underrightarrow{i_\mu} + \underrightarrow{i_r} = \left[\frac{1}{L_\mu} + \frac{1}{L_\sigma}\right] \cdot \underrightarrow{\psi_\mu} - \frac{1}{L_\sigma} \cdot \underrightarrow{\psi_r} \tag{3}$$

Torque can be given by two equations

$$T = \frac{3}{2} \cdot p \cdot Im\{\underrightarrow{\psi_\mu^*} \cdot \underrightarrow{i_s}\} \tag{4}$$

$$T = \frac{3}{2} \cdot p \cdot \frac{1}{L_\sigma} \cdot |\underrightarrow{\psi_\mu}| \cdot |\underrightarrow{\psi_r}| \cdot \sin\vartheta \tag{5}$$

with $\vartheta = \delta(\underrightarrow{\psi_\mu}) - \delta(\underrightarrow{\psi_r})$, p number of pole pairs. The first equation is used within the DSP program, the second is more suitable for basic deliberations. It is well known from the synchronous machine theory, and it will be taken to illustrate the basic idea of torque control.

3. Stator-Flux-Oriented Control

The basic task of machine control is to produce the demanded torque and to keep the (stator) flux on its demanded value.

Stator-flux-orientation leads the tip of the stator flux SV on a predetermined trajectory – which in case of high switching frequency is a multi-corner polygon, nearly a circle. The radius of the trajectory will be defined by control of the modulus of the stator flux SV; the tracking speed – in the sampled system the angular increment – results from the output of a torque controller [6]. In the following we assume that the modulation period T_m equal to the half switching period is small against to the rotor leakage time-constant $T_\sigma = L_\sigma/R_r$ and the fundamental period T_s.

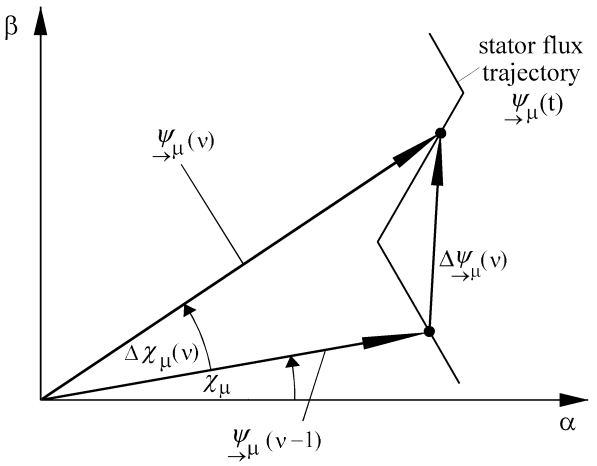

Fig. 2. Stator flux trajectory and stator flux increment $\underrightarrow{\Delta\psi_\mu}$ per modulation period υ

Fig. 2 shows the stator flux SV at the beginning and the end of a modulation period T_m (equal to processor cycle); in the most general case the stator flux is stretched by $k_\psi(v)$ and rotated by $\Delta\chi_\mu(v)$:

$$\psi_\mu(v) = \{(1 + k_\psi(v)) \cdot e^{j\Delta\chi_\mu(v)}\} \cdot \psi_\mu(v-1) \tag{6}$$

and thus changed by

$$\underrightarrow{\Delta\psi_\mu}(v) = \underrightarrow{\psi_\mu}(v) - \underrightarrow{\psi_\mu}(v-1) =$$

$$= \{(1 + k_\psi(v)) \cdot e^{j\Delta\chi_\mu(v)} - 1\} \cdot \underrightarrow{\psi_\mu}(v-1) \tag{7}$$

Fig. 3 shows the basic structure of the controller; $k_\psi(v)$ is delivered by a P-type flux modulus controller. The torque set (T^*) and actual value (T) are first transformed to slip angular frequencies by multiplication with $R_r/(3/2p \cdot \psi_r^2)$. Thus break-down can be easily prevented by limiting the set value. Then both values are compared in a PI-type controller delivering the dynamic part of the angular increment, $\Delta\chi_{\mu Dyn}$. The integral channel will be relieved by a stationary feed-forward

$$\Delta\chi_{\mu Stat} = (\omega + \omega_r^*) \cdot T_m \tag{8}$$

The following block calculates $\underrightarrow{\Delta\psi_\mu}(v)$ by expanding (7) in a Taylor series, broken after the fourth member:

$$\underrightarrow{\Delta\psi_\mu}(v) = k_\psi(v) \cdot \left\{1 - \frac{1}{2}\Delta\chi_\mu^2(v)\right\} \cdot \underrightarrow{\psi_\mu}(v-1) - \\ - \left\{\Delta\chi_\mu(v) - \frac{1}{6}\Delta\chi_\mu^3(v)\right\} \cdot \underrightarrow{\psi_\mu}(v-1) \tag{9}$$

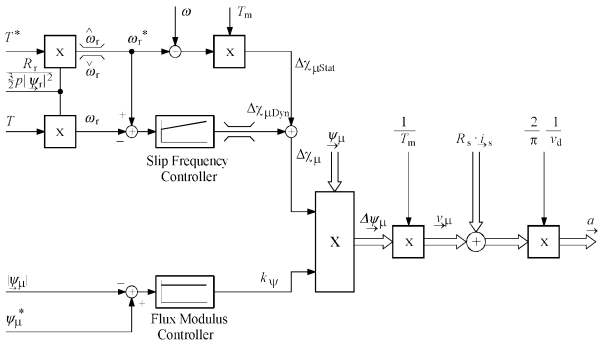

Fig. 3. Basic structure of Indirect StatorQuantities Control (ISC)

The stator flux increment SV will then be multiplied with $1/T_m$ yielding the magnetizing voltage $\underrightarrow{v_\mu}$, to which the resistive stator voltage drop $R_s \cdot \underrightarrow{i_s}$ will be added. Finally, division by $v_d \cdot \pi/2$ delivers the voltage control SV $\underrightarrow{a}$ handed to the PWM unit. Please, note that there are no underlaid current component controllers anymore!

The issue of low frequencies will be discussed in detail. The stator flux in the model will always be controlled correctly, even at zero frequency. But at low frequency the coincidence of model and real machine currents may be insufficient, mainly due to errors caused by the temperature-dependent stator resistance and of the inverter voltages modeled from measured DC link voltage v_d, and switching signals.

Fig. 4 shows the complete machine model acc. to equ. (1) ... (3). The very left blocks, in dashed lines, are current balancing controllers comparing measured ($i_{s\alpha(\beta)w}$) and model current ($i_{s\alpha(\beta)}$) coordinates, to correct these errors in a Luenberger observer structure. The gain has to be decreased with increasing speed, so that the model works as an *i-n*-model at low and as a *v-i*-model at high speed. If as already shown, the stator voltage drop is calculated with the model currents, the control acts only on the model, the true machine will only be "chained" to the model by the current balancing controllers. This enables e. g. testing of the control without powering the real drive.

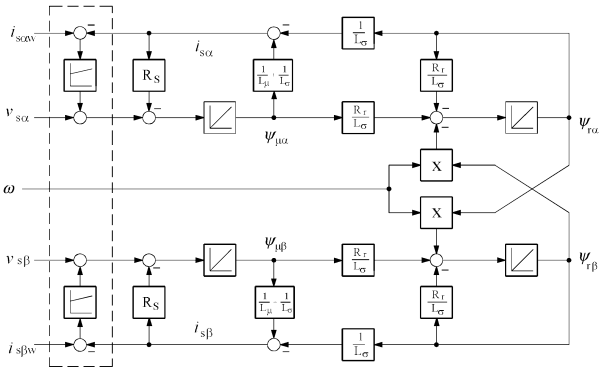

Fig. 4. Complete induction machine model (with current balancing controllers)

4. Field-Weakening Operation

For high power traction drives the limitation of output voltage by sinusoidal PWM to less than 90 % of the maximum possible value of the fundamental at square-wave modulation is disadvantageous as the break-down torque at high speed will be limited to less than 80 %. By means of suitable overmodulation schemes [7] some 95 % of the break-down torque can be reached, with comparable dynamics. But finally, the transition to square-wave modulation has to be performed. In the range of maximum voltage – it may be sinusoidal, "overmodulated" or square-wave – the torque (constant power range) can only be controlled by field-weakening.

Fig. 5 shows the completion of the control structure by a field-weakening controller.

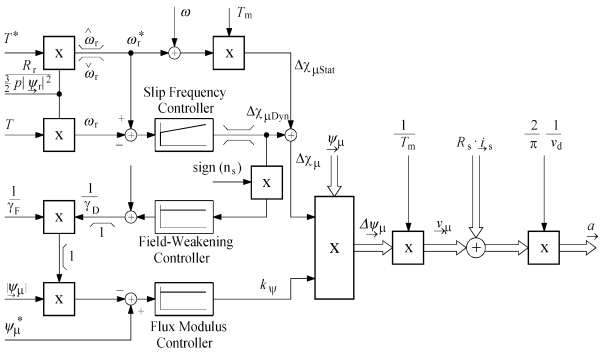

Fig. 5. Structure of ISC with Field-Weakening Controller

The stationary field-weakening via the factor $1/\gamma_F$ ($\gamma = \psi_\mu/\psi_{\mu rated}$; left part) works in forward mode by amplifying the flux modulus feed-back. The angular increase $\Delta\chi_\mu$ necessary for torque

increase cannot be gained as before, because the voltage is at its maximum. Here, Dynamic Field Weakening developed for DSC [1] is again helpful [6].

Fig. 6 shows the transient for a torque step out of idling operation, with the two stationary circular flux trajectories with radii γ_{EA} (before) and γ_{FC} (after the step). For short time the rotor flux SV moves further-on on the trajectory with the radius γ_{EA}, while the stator flux SV takes the „cut-off' trajectory AC having the same length as AB, weakening the stator flux modulus intermediately to γ_{min}. The angle ϑ is increased from zero to the sta-tionary value in the fastest possible way. The command for the dynamic field-weakening $1/\gamma_D$ is derived from the dynamic re-sponse of the slip frequency controller, $\Delta\chi_{\mu Dyn}$ increasing the flux feedback additionally.

A torque increase is thus performed in less than 1/3 of the fundamental period. At a negative torque step the dynamics are achieved only by variation of the control factor *a*. After that the stator flux modulus is guided rather slowly (taking into account the rotor leakage time-constant) to the stationary value, to avoid too big leakage flux and thus, over-current.

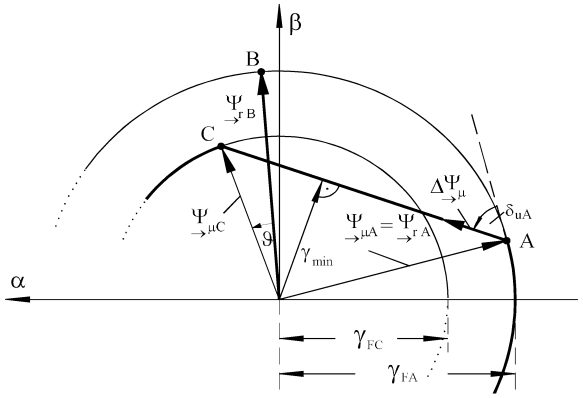

Fig. 6. Trajectories of stator and rotor flux SV at Dynamic Field Weakening

5. Correction of Inverter Voltage Errors

Each model-based control structure is as good as the quality of the modeled quantities and parameters. The major source of uncertainty is the modeling of the stator voltage from the measured DC link voltage and the switching signals. The errors are due to:

- Voltage drop across semiconductor devices
- Differences in the switching delay times
- Different influence of the interlocking time dependent on the sign of the inverter output (= stator) current
- Differences between motor and model ECD parameters

The first three error types depend mainly on the value and the sign of the inverter output current. In the structure described up to now the current coordinate balancing controller will compensate them, but only to the degree that is limited by the stability of the control.

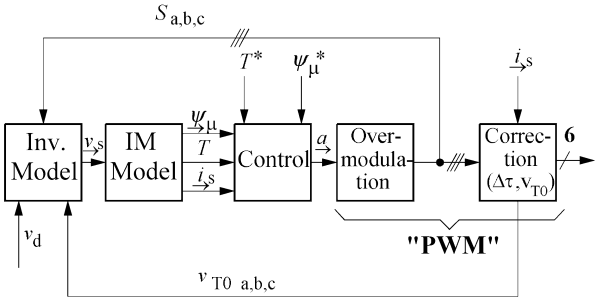

Fig. 7. Correction scheme for inverter errors in recent ISC

Fig. 7 shows the block structure of the correction system applied with ISC [7]; [9]. Control hands the set value for the stator voltage control SV to the Over-modulation block, where the zero sequence system for Symmetrized Sinusoidal Modulation is added and over-modulation is introduced, if needed.

In the Correction block the switching time errors are corrected and the device voltage drops is calculated, using the model stator current SV. Now the real switching edges will coincide with the ideal ones. The demanded switching commands $S_{a,b,c}$ are given back – together with the correction voltage drop signals – to the Inverter Model calculating the model stator voltages so that they are identical to those of the real motor.

It is now possible to operate the drive without current balancing controllers. The information set free by this can now be used to estimate, e.g. the speed. The most important ECD parameter at low frequency is stator resistance as it influences the stator current directly. It must be estimated on-line for high performance drives.

6. Sensorless Identification of Speed

Speed sensors in traction induction motors have always been a bottleneck as spoiling the robustness and/or control performance of the simple squirrel-cage motor: They are either robust – then the angular resolution is limited and the signal delay at low speed is high, or they have a high resolution and good dynamic re-sponse, but then, they are sensitive to shock and hazard.

In the last years the demand on the speed sensor has grown, e. g. for the aforementioned speed feed-forward or for speed control as a part of adhesion control systems. In low-floor Light Rail Vehicles the sensors considerably increase the volume of the individual small motors. Cost is not negligible for the sensor itself as well as for planning, mounting and commissioning, and is an important component of Life Cycle Cost.

Open-loop speed estimation schemes are already widely introduced in industrial applications. They are extremely dependent on parameters. Much more robust are observer schemes, as, e. g.

the one described in [8], which has been extended and specially improved by the following scheme ([7], [9], [10]).

The basis is the linear fundamental wave model used already in ISC; no parasitic effects as slotting or saliency are used. For purpose of investigation the real machine is described by an identical ECD; the quantities in the real machine will be designated by the index 'w'. The differences are $\Delta x = x - x_w$.

If both machine and model are fed by identical voltages as supposed and there is no difference in the parameters, the same current would flow in each. If the difference of the stator voltage drops is not too big at different speeds, both can be described in steady-state by the same Heyland circle diagram (Fig. 8).

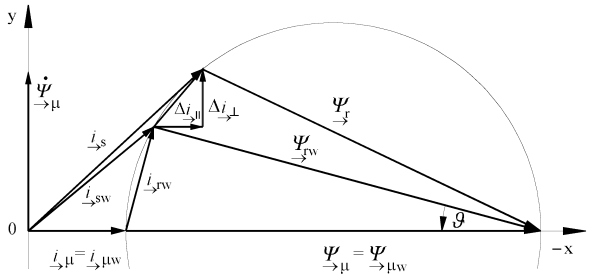

Fig. 8. Heyland Circle Diagram for real machine (x_w) and model (x), fed with identical voltages

It is obvious that the different speeds lead to different slip values and thus to different stator currents. If all other parameters are identical this difference can be employed to speed estimation. From the figure it can be seen that e. g. the component of $\underrightarrow{\Delta i_s}$ being perpendicular to the stator flux SV $\underrightarrow{\psi_\mu}$ will be suitable as indicator.

At the critical point of the stator frequency being zero the speed identification is not possible in the stationary state: The whole DC stator voltage drops over the stator resistance, the rotor mesh is short-circuited by the magnetizing inductance. Only a change of flux or speed can induce a current difference, which may be evaluated for speed identification.

The mathematical analysis of the stator current difference leads to a quasi differential equation of second order (12). To make it more compact some abbreviations and normalizations will be introduced. First, the time-constant factor:

$$\rho = \frac{L_\sigma + L_\mu}{L_\mu} \cdot \frac{R_s}{R_r} \tag{10}$$

and the leakage factor

$$\sigma = \frac{L_\sigma + L_\mu}{L_\mu}. \tag{11}$$

The rotational frequency is normalized to rotor breakdown angular frequency $\omega_{rb} = R_r/L_\sigma$ and designated by 'n', time is normalized to the inverse of ω_{rb}. The derivatives to the normalized time are marked by $\overset{\circ}{x}$. Then, the differential equation can be written as:

$$\underrightarrow{\overset{\circ\circ}{\Delta i_s}} + (\rho + 1 - j\, n_w) \cdot \underrightarrow{\overset{\circ}{\Delta i_s}} + (\rho - j\, n_w) \cdot \underrightarrow{\Delta i_s} =$$
$$= j \cdot \frac{1}{L_\sigma} \cdot [\Delta n \cdot \underrightarrow{\overset{\circ}{\psi}_r}] \tag{12}$$

The excitation of the system and by that the stator current difference vanishes if the following conditions are fulfilled:

- The speed difference or the rotor flux are permanently equal to zero (trivial case)
- The derivative of both quantities is zero. The last condition marks the case when speed identification fails at zero stator frequency.

In the stationary case under sinusoidal conditions the first and second time-derivative of the stator current difference can be expressed by the difference itself and the normalized stator frequency n_s:

$$\underrightarrow{\overset{\circ}{\Delta i_s}} = j \cdot n_s \cdot \underrightarrow{\Delta i_s}, \quad \underrightarrow{\overset{\circ\circ}{\Delta i_s}} = -n_s^2 \cdot \underrightarrow{\Delta i_s} \tag{13}$$

Then the solution of the differential equation for stationary operation is given by

$$\underrightarrow{\Delta i_s} = \frac{n_s}{[\rho\sigma - (n_r + \Delta n)n_s] + j \cdot [\rho(n_r + \Delta n) + n_s]} \cdot$$
$$\cdot \frac{\Delta n}{L_\sigma} \cdot \underrightarrow{\psi_r} \tag{14}$$

This is a rotating space vector containing the information about the speed difference. After multiplication with the conjugate complex rotor flux SV, the leakage inductivity L_σ, an additional suited working-point-dependent complex factor $\underline{K}$ and division by Ψ_r^2 a resting quantity is obtained. The real part is parallel and the imaginary part perpendicular to the product of $\underrightarrow{\psi_r}$,. and $\underline{K}^*$.

$$Im\left\{\frac{\underrightarrow{\psi_r^*}}{\psi_r^2} \cdot \underline{K} \cdot \underrightarrow{\Delta i_s} \cdot L\sigma\right\} = G_{i2} \cdot \Delta n \tag{15}$$

The perpendicular component to be used for speed identification in an observer structure is proportional to the speed difference and a function of the machine and operating parameters and will be summarized in a factor G_{i2}. In the prevailing operation range the factor $\underline{K}$ is chosen equal to

$$\underline{K} = (1 + j \cdot n_r/\sigma)/\sqrt{1 + n_r^2}, \tag{16}$$

showing a rather uniform negative gain. Only in the range of very low stator frequency with opposite signs of torque and speed the indicator would change its sign [9] and defeat a stable control. The factor is then to be chosen as shown in [10] to

$$\underline{K} = (1 + j \cdot n_r/\sigma)/\sqrt{1 + (n_r/\sigma)^2} \tag{17}$$

That case is depicted in Fig. 9 dependent on stator frequency n_s, up to about double rated speed, with the normalized slip frequency n_r as the main parameter.

At the critical zero stator frequency the indicator G_{i2} vanishes in both cases, the machine is unobservable. Outside this region

the left part of equ. (15) can be used as error function for a PI-controller adjusting the speed signal in the observer. The practical settling time is about one third of the rotor leakage time-constant T_σ [9].

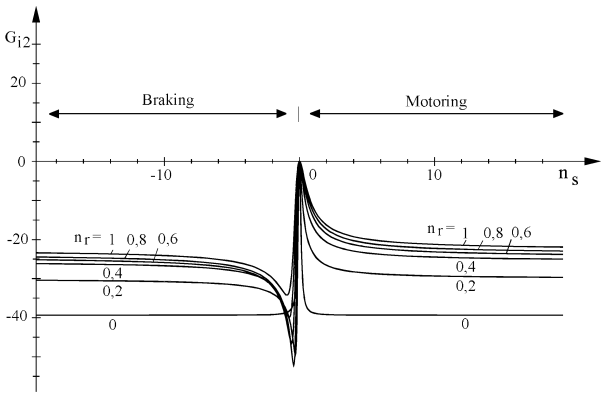

Fig. 9. Factor $G_{i2} = f(n_s, n_r)$; equ. (17)

The excellent quality of this speed observer scheme will be demonstrated by experimental results of a 120 kW traction motor fed from a 500 kVA IGBT traction inverter with a nominal d. c. link voltage of 750 V.

Fig. 10 shows the speed estimation under dynamic conditions. If a torque set value step sequence is applied to the induction machine coupled with a DC machine, speed follows mainly in a triangular fashion. Real speed ω_w. (measured with an incremental encoder with 2000 pulse/rev.) and estimated speed ω are shown, together with the torque functions.

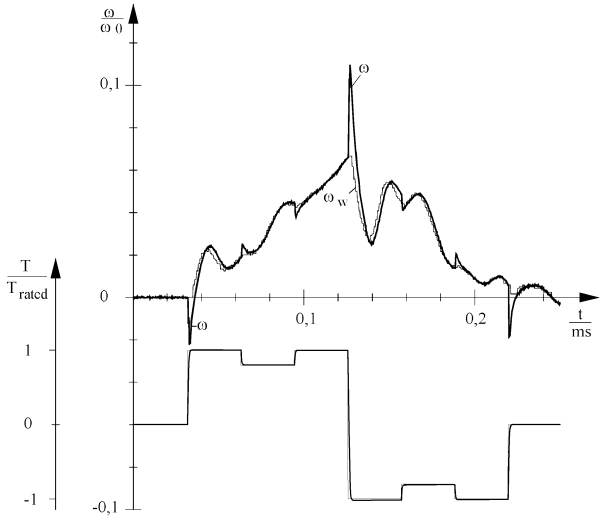

Fig. 10. Estimated (ω) and measured speed (ω_w) at acceleration and braking with up to 100 % rated torque

Estimated speed follows the measured speed astonishingly exactly, including the oscillation of the two-masses-spring-system.

The peaks in ω when the torque changes very fast are due to the current displacement effects in the rotor bars reducing L_σ. So the real rotor currents rise faster than those in the model, whichdoes not take into consideration this effect. This will be interpreted by the speed observer as a negative speed error. It has no vital consequence on the quality of speed estimation as the set value and actual torque differ anyway during such extremely fast transients.

With such a scheme speed reversals with a change rate of 24 min^{-1}/s and permanent full load operation at minimum stator frequency of only 0.33 Hz can be safely managed. But it must be kept in mind that at still lower values or rates of change the scheme will fail. An escape of the problem will be given in sect. 8.

7. Stator Resistance Estimation

An indispensable prerequisite is exact on-line identification of the stator resistance which changes severely with temperature. Obviously thermal sensors are not wanted.

The same change of temperature in stator and rotor shall be assumed as the first approach. So, the value of ρ does not change when R_s changes. Then an equation similar to (14) can be found for the appertaining stator current SV difference caused by the difference ΔR_s [11]. For small values of ΔR_s and $\rho = \rho_w$ this equation can be written as:

$$\underrightarrow{\Delta i_s}_R = \frac{n_r^2 - \sigma^2 - j \cdot 2\sigma n_r}{\underline{Z}} \cdot \frac{\Delta R_s}{L_\sigma \cdot R_r} \cdot \underrightarrow{\psi_r} \qquad (18)$$

with

$$\underline{Z} = [\rho \cdot \sigma - n_r \cdot n_s] + j \cdot [\rho \cdot n_r + n_s]\,. \qquad (19)$$

Multiplying the sum of equ. (14) and equ. (18) with the conjugate-complex rotor flux SV, L_σ, the complex (mainly imaginary) factor $\underline{Z}$ and $1/\Psi_r^2$ yields again a resting quantity. The imaginary part of this is proportional to ΔR_s:

$$Im\left\{\frac{\underrightarrow{\psi_r^*}}{\psi_r^2} \cdot (\underrightarrow{\Delta i_s} + \underrightarrow{\Delta i_s}_R) \cdot L\sigma \cdot \underline{Z}\right\} = G_{Rs} \cdot \frac{\Delta R_s}{R_r} \qquad (20)$$

In steady state Δn has no influence on the result, as it contains the real part only. As the stator resistance changes only slowly an integral controller will be used for identification. The left side of equ. (20) multiplied by the sign of n_r, is taken as its input. This method is independent of the speed identification scheme for small differences of speed and stator resistance.

Fig. 11 shows that speed estimation at very low stator frequency needs to correct the values of R_s. The drive (the same as in Fig. 10) operates at standstill with 100 % rated torque (= 35% of breakdown torque T_b). The model stator resistance value is initialized to 80 % of its nominal value. Due to this mismatch the estimations of the stator flux and, correspondingly, those of the speed are wrong. The ripple frequency is six times the stator fre-

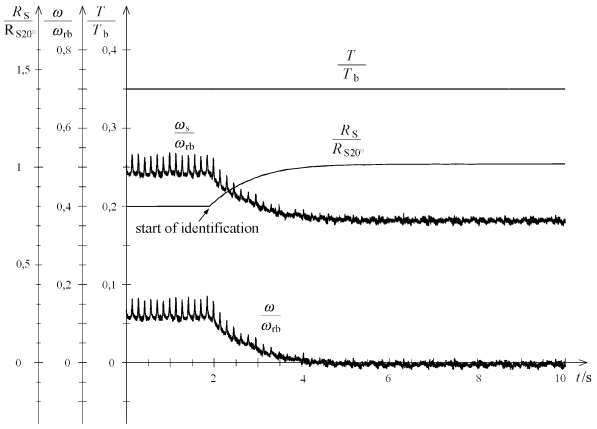

Fig. 11. On-line identification of stator resistance at standstill

quency due to malfunctioning of the inverter correction circuit (Fig. 7) by a severe difference between $\underrightarrow{\Delta i_s}$ and $\underrightarrow{\Delta i_{sw}}$. The initial error in speed is 1 % of rated speed. At $t = 1.9$ s the identification of R_s starts, the actual value of 1.018 $R_{s20°C}$ is found within 2 ... 3 s. Simultaneously, all state variables converge to their correct values, the ripple vanishes and speed reaches the correct zero value. The method operates well in the range of small frequencies where the influence of the stator resistance is relevant (and where this identification is necessary).

8. Operation with Infinitely Slow Change between Driving and Braking

The speed of a linearly modeled induction machine cannot be observed at zero stator frequency without injecting test signals providing a change of flux. The test signals are often not wanted as they may be disturbing or cannot be injected sufficiently with the low switching frequency of high power inverters.

As it has been shown that slow transients through the region of very low stator frequencies can be safely managed, the question is whether an operation mode is possible which simply avoids stationary working in the region below 0.4 ... 0.5 Hz (a value that can safely be mastered with the described control structure).

To that purpose a scheme has been proposed and successfully implemented [11] which avoids operation with too low stator frequency by manipulating the stator flux modulus. For a given (non-zero) torque a reduction of the rotor flux modulus increases the necessary slip frequency:

$$\omega_r = \frac{R_r \cdot 2}{3 \cdot p \cdot \psi_r^2} \cdot T \qquad (21)$$

The function of the operation management is explained for the reversion of speed at constant torque. Fig. 12 shows the normalized slip frequency n_r as a function of normalized speed. In the diagram, the working points with constant normalized stator frequency n_s are joined by straight lines with gradient -1. Speed identification works safely for stator frequencies with an absolute value $\geq \check{n}_s$. Thus the drive must not work stationarily in the region between the lines $n_s = -\check{n}_s$ and $n_s = \check{n}_s$ in Fig. 12.

Starting at point A, the machine brakes with negative speed and positive (non-zero) torque and slip frequency; the absolute values of speed and stator frequency decrease. At point B the stator frequency reaches its limit $n_s = -\check{n}_s$.

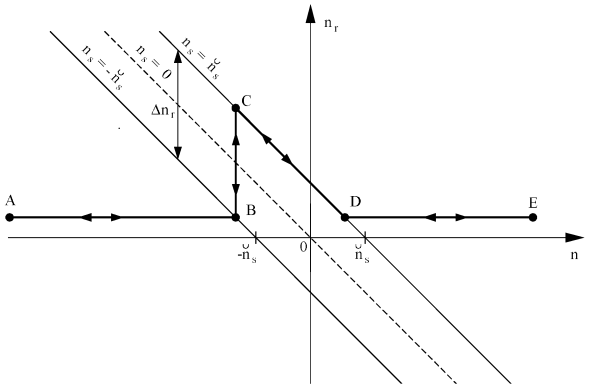

Fig. 12. Normalized slip frequency n_r vs. normalized speed n at constant torque

Now, there are two choices to produce the wanted torque: With full flux, minimal slip frequency and negative stator frequency (point B) or with reduced flux magnitude and a slip frequency increased by Δn_r, (point C), where the stator frequency is already positive and $\geq +\check{n}_s$. The operation management decides to decrease the flux so that the crossing of the stator frequency through the "forbidden zone" is sufficiently fast. On the other hand, the transition must be slow with regard to the rotor leakage time-constant T_σ, to avoid an inadmissibly dynamic increase of the leakage flux and thus stator current.

As speed further changes, the operation point moves along the line $n_s = +\check{n}_s$ towards point D, while the flux is continuously increasing again, so that the drive is operated with maximum permissible flux and minimum stator current. This is done by stator frequency control. At point D normal motoring operation with full flux and constant slip frequency is reached again and maintained until point E.

The opposite reversing starts at point E in the motoring mode. With decreasing speed point D and $n_s = +\check{n}_s$ is reached. For further decreasing speed the flux must be decreased continuously to keep the stator frequency at its upper limit $+\check{n}_s$. The control supervises whether the torque can be produced with full flux and negative stator frequency $\leq -\check{n}_s$, too. When the condition is fulfilled at point C, the drives change sharply to point B.

In practical operation an additional hysteresis avoids jittering. Fig. 13 shows the time functions of such a very slow speed reversal, measured at the 120 kW drive. The load machine is speed-controlled and impresses the triangularly changing speed.

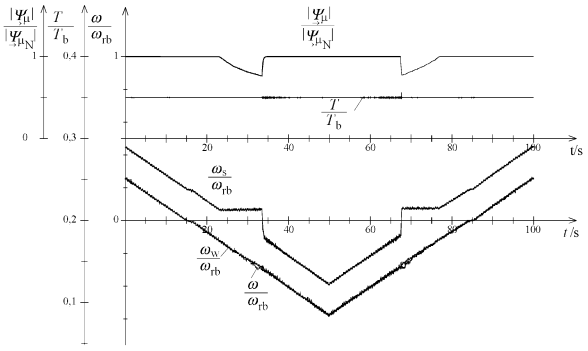

Fig. 13. Very slow speed reversing operation with rated torque. 120 kW motor.

The two upper traces show stator flux modulus and torque, in the middle there is the observed stator frequency and the lower traces slow the nearly perfectly coinciding values of true and observed speed. For $T_{rated} = 0.35\ T_b$. The rated slip frequency is 0.187 ωr_b, = $2\pi \cdot 0.89$ 1/s, which is more than the double of $\breve{\omega}_s = 2 \cdot \pi \cdot 0.331$/s ; the frequency hysteresis is 0.02 ωr_b. Stator flux is reduced down to 50 %.

[11] shows how at no-load condition safe transition is reached by switching on a minimum torque of less than 3.5 % of rated torque. [12] reports on practical tests on a Combino® low-floor tram. It shows that vehicles running down a slope can be smoothly stopped, held at zero speed and accelerated in the opposite direction, without speed sensors.

9. Conclusion

Indirect Stator-Quantities Control (ISC) unifies the advantages of stator-flux-orientation proven successful in Direct Self Control with Pulse Width Modulation that is well suitable for fast-switching IGBT inverters. Using the signals available in the control model motor speed can be estimated so that no speed sensors are needed anymore. With careful correction of inverter voltage errors stator voltage sensors are not necessary. Additional work not described here has been necessary for automatic parameter identification of machine and inverter model and for procedures of magnetizing the machine with unknown speed and residual flux without speed-sensor.

10. References

[1] STEIMEL, A.: *Control of the Induction Machine in Traction*. 8th International Power Electronics and Motion Control Conference (PEMC' 98), Prague 1998, K 4 & Elektrische Bahnen 96 (1998), No. 12, 361–369

[2] DEPENBROCK, M.: *Direct Self-Control (DSC) of Inverter-Fed Induction Machine*. IEEE Transactions on Power Electronics, 1988, No. 4, 420–429

[3] STEIMEL, A.: *Steuerungsbedingte Unterschiede von wechselrichtergespeisten Traktionsantrieben*. Elektrische Bahnen 92 (1994), No. 1/2, 24–36.

[4] JÄNECKE, M.; KREMER, R.; STEUERWALD, G.: *Direct Self Control (DSC), A Novel Method Of Controlling Asynchronous Machines in Traction Applications.* Elektrische Bahnen 88 (1990), No. 3, 81–87

[5] KOVÁCS, K. P.; RÁCZ, L: *Transiente Vorgange in Wechselstrommaschinen*. Verlag der Ungarischen Akademie der Wissenschaften, Budapest 1959.

[6] JÄNECKE, M.; HOFFMANN, F.: *Fast Torque Control of an IGBT-Inverter-Fed Three-Phase A. C. Drive in the Whole Speed Range - Experimental Results*. 6th EPE Conference 1995, Sevilla,Vol. 3, 399–404

[7] HOFFMANN, F.: *Drehgeberlos geregelte Induktionsmaschinen an IGBT-Pulsstromrichtern.* Ph. D. Thesis Ruhr-Universitat Bochum 1996. Fortschr.- Ber. VDI Reihe 21 Nr. 213, Diisseldorf 1996

[8] KUBOTA, H.; MATSUSE, K.; NAKANO, T.: *DSP-Based speed adaptive flux observer of induction motor*. IEEE Trans. on Industry Applications, 1993, No. 2, 344-348

[9] DEPENBROCK, M.; HOFFMANN, F.; KOCH, ST.: *Speed Sensorless High Performance Control For Traction Drives.* 7th EPE Conference 1997, Trondheim, Vol. l, 1.418–1.423

[10] Hoffmann, F.; Koch, St.: Steady State Analysis of Speed Sensorless Control of Induction Machines. IECON'98 (Aachen), Vol. 3, 1626–1631

[11] DEPENBROCK, M.; FOERTH, CH.; KOCH, ST.: *Speed Sensorless Control Of Induction Motors At Very Low Stator Frequencies*. 8th EPE Conf. 1999, Lausanne

[12] FRENZKE, T.; HOFFMANN, F.; LANGER, H. G.: *Speed Sensorless Control of Traction Drives - Experiences on Vehicles*. 8th EPE Conference 1999, Lausanne